ICSV14
Cairns • Australia
9-12 July, 2007

SOMETIMES DIGITAL CONTROL LEADS TO CHAOS

Gábor Csernák[1]*, Gábor Stépán[2]†

[1]HAS-BUTE Research Group on Dynamics of Machines and Vehicles
H-1521 Budapest, Hungary

[2]Budapest University of Technology and Economics
Department of Applied Mechanics
H-1521 Budapest, Hungary

csernak@mm.bme.hu
stepan@mm.bme.hu

Abstract

In the present paper, we introduce and analyse a mechanical system in which the digital implementation of a linear control loop may lead to chaotic behaviour. The amplitude of the evolving oscillations is usually very small, this is why these are called micro-chaotic vibrations. As a consequence of the digital effects, i.e., the sampling and the round-off error, the behaviour of the system can be described by a three dimensional piecewise linear map, the micro-chaos map. We examine a 2D version of the micro-chaos map and prove that the map is chaotic.

1. INTRODUCTION

Even the application of a linear control law may lead to chaotic behaviour if there is some nonlinearity in the implementation of the control system – digital control is an eminent example for this case –, or state-dependent delayed control is applied [1].

In the present paper, we analyse a simple model of a digitally controlled mechanical system, which may perform chaotic vibrations. As a consequence of the digital effects, i.e., the sampling and the round-off error, the behaviour of this system can be described by a piecewise linear map, the micro-chaos map [2]. It was proved in the mid-nineties by Haller and Stépán [3] that the 1D version of the micro-chaos map is chaotic. A couple of years later we found that if dry friction is present in the system, the resulting behaviour is transient chaotic. We developed methods for the determination of the mean lifetime of chaotic transients in the case of the 1D piecewise linear micro-chaos map [4, 5]. The goal of our present contribution is to perform the first step of the same program for a 2D version of the map, i.e., we prove that the map is chaotic.

2. FUNDAMENTAL PROPERTIES OF THE 2D MICRO-CHAOS MAP

2.1. Derivation of the 2D micro-chaos map

The mechanical model of a digitally controlled polishing tool is shown in Figure 1. The characteristic of the friction force between the revolving polishing tool and the fixed workpiece is a mixture of the dry and viscous friction characteristics. Consequently, to stabilize the tool in a certain position, control force must be applied. The shaft of the polishing tool is driven by a DC motor, which exerts a control force Q, governed by a digital control system. The linearized,

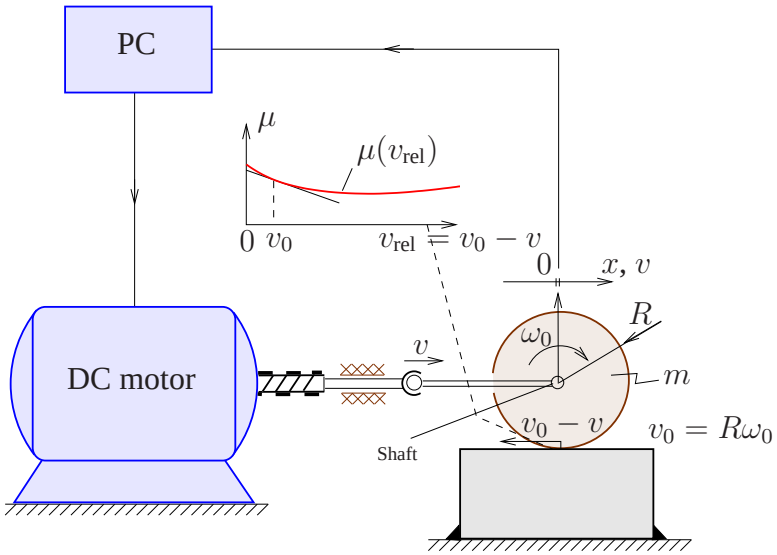

Figure 1. The mechanical model of the polishing tool

first order equation of motion of the system assumes the following form:

$$m\dot{v} + mg\mu'(v_0)v = mg\mu(v_0) \underbrace{-mg\mu(v_0) - Dv}_{Q\text{: control force}}. \tag{1}$$

The computer samples the velocity v at discrete time instances, $v_j \equiv v(t_j) \equiv v(j\tau)$, $j \in \{1, 2, \dots\}$; $t_j = j\tau$ is the j^{th} sampling instant, τ is the sampling time. Since some time is needed to process the measured signal, the force is exerted by the motor a bit after the sampling instant. We assume that this processing delay is equal to the sampling time. In this case the control force exerted at t_j depends on the data sampled at t_{j-1}.

Since the output signal has a finite resolution, h, the behaviour of this system can be described by the following 2D map:

$$\begin{bmatrix} v_{j+1} \\ u_{j+1} \end{bmatrix} = \begin{bmatrix} a & 1 \\ 0 & 0 \end{bmatrix} \begin{bmatrix} v_j \\ u_j \end{bmatrix} - \begin{bmatrix} 0 \\ bh\text{Int}\left(\frac{Dv_j}{h}\right) \end{bmatrix}, \tag{2}$$

where u_j corresponds to the control force exerted at t_j,

$$a = e^{fg\tau}, \quad b = \frac{D}{fmg}\left(e^{fmg} - 1\right), \quad \text{and} \quad f = -\mu'(v_0) > 0. \tag{3}$$

Introducing the new variable $y_j = Dv_j/h$, Equation (2) can be rewritten as

$$y_{j+1} = ay_j - b\,\mathrm{Int}(y_{j-1}). \tag{4}$$

Taking into account the effect of sampling but disregarding the round-off error, the corresponding map assumes the following form:

$$y_{j+1} = ay_j - by_{j-1}. \tag{5}$$

In this case the origin is the single fixed point, which – according to the Jury criterion, i.e., the transformed Routh-Hurwitz criterion – is stable if

$$(a,b) \in G = \left\{(\alpha,\beta) \in \mathbb{R}^2 |\ a > 1, b < 1, a - b < 1\right\}. \tag{6}$$

Note, that these criterions imply that $a < 2$. During the analysis of (4), we will restrict ourselves to the parameter domain G, and examine cases when the solution is positive ($y_{j-1} > 0$, $y_j > 0$). Our results can be naturally extended to the case of negative solutions, too.

2.2. Fixed points

In case of the map (4), there may exist several fixed points. Divide the plane (y_{j-1}, y_j) into parallel bands:

$$M_m = \{(y_{j-1}, y_j) \mid m \le y_{j-1} < m + 1\} \quad \text{if} \quad m > 0, \text{ and} \tag{7}$$

$$M_0 = \{(y_{j-1}, y_j) \mid -1 < y_{j-1} < 1\}. \tag{8}$$

There can be at most one fixed point in each band: $\bar{\mathbf{p}}^m = (\bar{y}^m, \bar{y}^m)$, where

$$m \le \bar{y}^m = \frac{mb}{a-1} < m + 1 \quad \text{if} \quad m \ge 0. \tag{9}$$

2.3. Basic branches

As it can be shown easily, the fixed points are hyperbolic with the eigenvalues $\lambda_1 = 0$ and $\lambda_2 = a > 1$. The unstable manifold (unstable line) of the fixed point $\bar{\mathbf{p}}^m$ can be given as $U_m : y_j = ay_{j-1} - bm$. Since $\lambda_1 = 0$, the solution immediately arrives at the family of the unstable lines U_m, $m = 0, 1, 2, \ldots$, and stays on these lines.

The intersection point of U_m and the line $y_{j-1} = m$ is $\mathbf{p}^m_m = (m, y^m_m) = (m, (a-b)m)$, while the intersection point of U_m and the line $y_{j-1} = m + 1$ is $\mathbf{p}^m_{m+1} = (m + 1, y^m_{m+1}) = (m + 1, a(m + 1) - bm)$. The upper index refers to the number of the unstable line while the lower index shows the first coordinate of the point. Since points in the mth band are mapped onto the unstable manifold of $\bar{\mathbf{p}}^m$, the image of $\mathbf{p}^m_m$: $\mathbf{p}^m_{\text{inf}} = (x^m_{\text{inf}}, y^m_{\text{inf}}) = ((a-b)m, (a^2 - ab - b)m)$ is the leftmost point that can be reached from U_m. Since $\mathbf{p}^m_{m+1} \in M_{m+1}$, its image $\mathbf{p}^m_{\text{sup}} = (x^m_{\text{sup}}, y^m_{\text{sup}}) = ((a-b)m + a, (a^2 - ab - b)m + a^2)$ is the rightmost accumulation point of the points that can be reached from U_m. According to these results, the basic branch of the fixed point $\bar{\mathbf{p}}^m$, i.e., the longest piece of the manifold emanating from the fixed point, is defined as

$$y_j = ay_{j-1} - bm, \quad (a-b)m \le y_{j-1} < (a-b)m + a. \tag{10}$$

As computer experiments showed, there are finite domains in the parameter plane (a, b), where the solution stays on the fundamental branches of certain fixed points. These fundamental branches form the attractor of the system – see Figure 2.

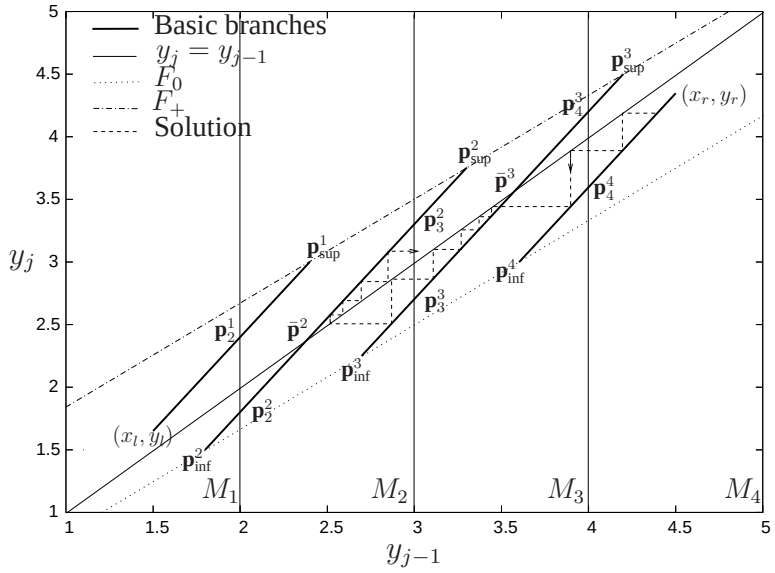

Figure 2. Attractor of the 2D micro-chaos map, $a = 1.5, b = 0.6$

Note that if we neglect the processing delay, we arrive at the following 1D map:

$$y_{j+1} = ay_j - b\,\text{Int}(y_j). \tag{11}$$

This map is chaotic as it was proved in [3]. The graph of (11) is shown in Figure 3. As it can be seen, the graph of (11) is similar to the attractor of (4).

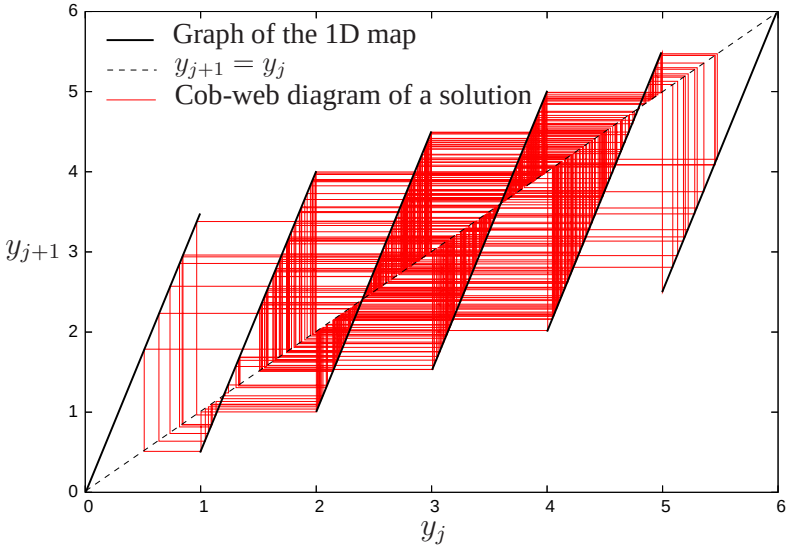

Figure 3. 1D micro-chaos map, $a = 3.5,\ b = 3.0$

Based on this similarity, the successive iteration steps of the 2D map (4) can be followed easily on a modified cob-web diagram. Starting at a certain initial point, the next point is found

as follows: one projects the point "horizontally" to the diagonal, then "vertically" to the line of the attractor. In the "multi-valued" domains the appropriate branch is selected according to the previous value of the coordinate y_{j-1}.

The solution can jump from the mth basic branch to the next one, over the corresponding fixed point, if $y_{\text{sup}}^m > \bar{y}^{m+1}$. This situation may occur if

$$b < \frac{a^2(a-1)(m+1)}{ma^2+1}. \tag{12}$$

Similarly, the condition of $y_{\text{inf}}^m < \bar{y}^{m-1}$ is

$$b > \frac{a^2(a-1)m}{ma^2-1}. \tag{13}$$

If these conditions are not fulfilled, the basic branches of $\bar{\mathbf{p}}^{m+1}$ or $\bar{\mathbf{p}}^{m-1}$ become mangled, since the solution cannot go to the other side of the corresponding fixed point.

Thus, the maximal and minimal numbers m, with which whole basic branches occur are

$$m_{\text{min}} = \text{Int}\frac{b}{a^2(b+1-a)} \quad \text{and} \quad m_{\text{max}} = \text{Int}\frac{a^2(a-1)-b}{a^2(b+1-a)} + 1. \tag{14}$$

The rightmost point of the attractor can be obtained as the image of $y_{\text{sup}}^{m_{\text{max}}}$:

$$(x_r, y_r) = (a(a-b)-b)m_{\text{max}} + a^2, ax_r - b(m_{\text{max}}+1)). \tag{15}$$

The leftmost point of the attractor can be obtained as the image of $y_{\text{inf}}^{m_{\text{min}}}$:

$$(x_l, y_l) = (a(a-b)-b)m_{\text{min}}, ax_l - b(m_{\text{min}}-1)). \tag{16}$$

The introduced points are shown in Figure 2, together with the auxiliary lines $F_0: \; y_j = \frac{a^2-ab-b}{a-b}y_{j-1}$ and $F_\pm: \; y_j = \frac{a^2-ab-b}{a-b}y_{j-1} \pm \frac{ab}{a-b}$, passing through the endpoints of the basic branches.

3. PROOF OF CHAOS

In this section we will prove that map (4) has chaotic solutions in certain parameter domains.

3.1. Sensitive dependence on initial conditions

We know that solutions arrive at the family of unstable lines $y_j = ay_{j-1} - mb$, $m = 0, 1, 2, \ldots$, and stay on these lines. The distance of two neighbouring lines is $b/\sqrt{1+a^2}$.

Let us fix a constant $\delta = b/(1+a^2) < b/\sqrt{1+a^2}$. We will show that for any two points $\mathbf{p_0} \neq \mathbf{q_0}$ with $|\mathbf{p}_0 - \mathbf{q}_0| < \delta$, there exists $N \geq 1$ such that the distance of the Nth iterates of these points is less than δ:

$$|\mathbf{p}_N - \mathbf{q}_N| \geq \delta. \tag{17}$$

According to the conditions stated above, $\mathbf{p}_0$ and $\mathbf{q}_0$ must lie on the same line and if they arrive at different lines, we are done. Since the map exponentially expands the distances of

points taken from the same band and the same line, without loss of generality we can assume that after n iterations the two points arrive at different bands. If $|\mathbf{p}_n - \mathbf{q}_n| \geq \delta$, we are done. If not, then we have $|\mathbf{p}_n - \mathbf{q}_n| < \delta = b/(1+a^2) < 1$, thus, we can assume that $\mathbf{p}_n = (u, au - mb) \in M_i$ and $\mathbf{q}_n = (v, av - mb) \in M_{i+1}$. The next iterates of these points are $\mathbf{p}_{n+1} = (au - mb, a(au - mb) - ib)$ and $\mathbf{q}_{n+1} = (av - mb, a(av - mb) - (i+1)b)$. Consequently,

$$|\mathbf{p}_{n+1} - \mathbf{q}_{n+1}| = |(a(u-v), a^2(u-v) - b)| > |(0, a^2(u-v) - b)| > b - a^2|v-u| > b - a^2\delta = \delta. \tag{18}$$

Hence the choice $N = n + 1$ completes the proof.

3.2. Existence of an attractor

Under certain conditions – e.g., $y^m_{\text{sup}} < y^{m+1}_{m+2}$ and $y^m_m < y^m_{\text{inf}}$ –, it follows from the definition of the points introduced in Section 2.3 that there are broad parameter domains where the basic branches between (x_l, y_l) and (x_r, y_r) form an invariant and attractive set $\mathcal{A}$. More precisely, the attractor consists of segments of the lines $y_j = ay_{j-1} - bi$, where

$$y_{j-1} \in (x_l, x^{m_{\text{min}}-1}_{\text{sup}}), \quad i = m_{\text{min}} - 1 \tag{19}$$
$$y_{j-1} \in (x^{m_{\text{min}}}_{\text{inf}}, x^{m_{\text{min}}}_{\text{sup}}), \quad i = m_{\text{min}} \tag{20}$$
$$\vdots$$
$$y_{j-1} \in (x^{m_{\text{max}}}_{\text{inf}}, x^{m_{\text{max}}}_{\text{sup}}), \quad i = m_{\text{max}} \tag{21}$$
$$y_{j-1} \in (x^{m_{\text{max}}+1}_{\text{inf}}, x_r), \quad i = m_{\text{max}} + 1. \tag{22}$$

As an example, see Figure 2, where $m_{\text{min}} = 2$ and $m_{\text{max}} = 3$. The set

$$y_{j-1} \in (m_{\text{min}} - 1, m_{\text{min}}), \quad y_j \in (\bar{y}^{m_{\text{min}}-1}, y^{m_{\text{min}}-1}_{m_{\text{min}}}) \tag{23}$$
$$y_{j-1} \in (m_{\text{min}}, m_{\text{min}} + 1), \quad y_j \in (y^{m_{\text{min}}}_{m_{\text{min}}}, y^{m_{\text{min}}}_{m_{\text{min}}+1}) \tag{24}$$
$$\vdots$$
$$y_{j-1} \in (m_{\text{max}}, m_{\text{max}} + 1), \quad y_j \in (y^{m_{\text{max}}}_{m_{\text{max}}}, y^{m_{\text{max}}}_{m_{\text{max}}+1}) \tag{25}$$
$$y_{j-1} \in (m_{\text{max}} + 1, m_{\text{max}} + 2), \quad y_j \in (y^{m_{\text{max}}+1}_{m_{\text{max}}+1}, \bar{y}^{m_{\text{max}}+1}) \tag{26}$$

is part of the basin of attraction of $\mathcal{A}$.

There are cases when the attractor consists of only two mangled basic branches. In such cases Equations (14) lead to $m_{\text{min}} = m_{\text{max}} + 1$, Although these numbers cannot be interpreted as the indices of the leftmost and rightmost whole basic branches, the above expressions still hold.

3.3. Topological transitivity

It this section we show that in certain parameter domains the attractor $\mathcal{A}$ can be partitioned in such a way that any region can be reached from any other region in a finite number of steps. Introduce the transition matrix A of the partition as

$$a_{ij} = \begin{cases} 1 & \text{if } \overline{F(I_i)} \supset I_j \\ 0 & \text{otherwise} \end{cases}. \tag{27}$$

We will show via an example that the transition matrix, describing the dynamics over the partition, is primitive, i.e., there exists an integer number $n > 0$, such that every element of A^n is positive. Consequently, the matrix is irreducible, as well.

The attractor of map (4) can be seen in Figure 4 at parameters $a = 1.25$ and $b = 0.6$. The

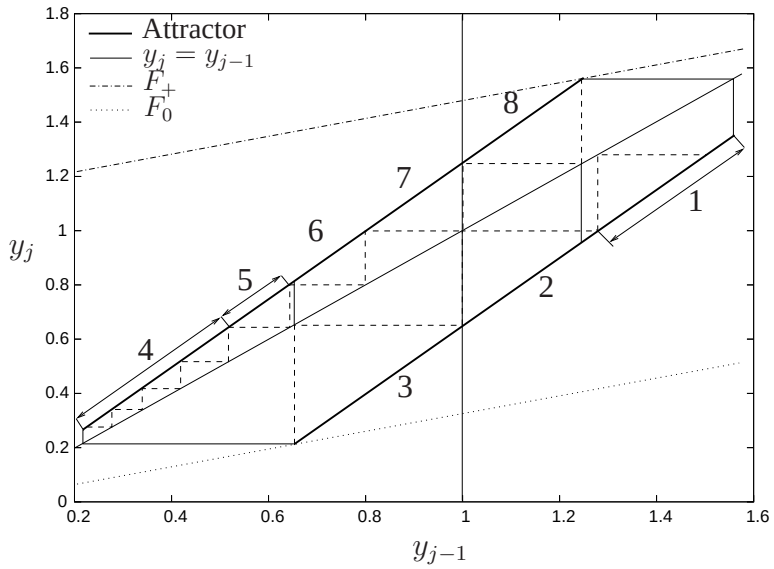

Figure 4. Partition of the attractor, $a = 1.25$, $b = 0.6$

partition of the attractor is constructed as follows: the sections between the $y_{j-1} = 1$ line and the F_0 or F_+ lines are the basic regions. These are denoted by 3 and 8 in Figure 4. The pre-images of these segments form the remaining regions. As it can be seen in Figure 4, the third pre-image of region 3 would stretch out from the basic branch, this is why region 1 consists of the pre-image of region 2 and the remaining part of the basic branch. Important that this way the image of 8 fully covers region 1. On the other basic branch, region 4 consists of certain pre-images of region 5 and the remaining part of the basic branch. As it can be observed, the image of region 3 fully covers regions 4 and 5. According to this partitioning, every region can be reached from any other region. The transition matrix of this partition can be written as follows:

$$\mathbf{A} = \begin{bmatrix} 0 & 1 & 0 & 0 & 0 & 0 & 0 & 0 \\ 0 & 0 & 1 & 0 & 0 & 0 & 0 & 0 \\ 0 & 0 & 0 & 1 & 1 & 0 & 0 & 0 \\ 0 & 0 & 0 & 0 & 1 & 0 & 0 & 0 \\ 0 & 0 & 0 & 0 & 0 & 1 & 0 & 0 \\ 0 & 0 & 0 & 0 & 0 & 0 & 1 & 0 \\ 0 & 0 & 0 & 0 & 0 & 0 & 0 & 1 \\ 1 & 0 & 0 & 0 & 0 & 0 & 0 & 0 \end{bmatrix}. \tag{28}$$

There are finite parameter domains where the structure of the partition and the $m \times m$ transition matrix is similar to the one shown in the example, i.e., there is one non-zero element in every

row and column, not in the main diagonal, and there is an additional non-zero element a_{kj}:

$$a_{ii+1} = 1, \quad i = 1 \dots m-1 \tag{29}$$

$$a_{m1} = 1 \tag{30}$$

$$a_{kj} = 1, \quad \text{where } k \neq j,\ k+1 \neq j. \tag{31}$$

It can be shown, that in this case $A^2_{k-1j} > 0$ if $k > 1$, or $A^2_{mj} > 0$ if $k = 1$, and $A^2_{kj+1} > 0$ if $j < m$, or $A^2_{k1} > 0$ if $j = m$. Thus, the existence of the additional non-zero element a_{kj} implies the appearance of two additional non-zero elements. Moreover, $A^2_{ii+2} > 0$ if $i < m-1$, or $A^2_{i1} > 0$ if $i = m-1$, or $A^2_{i2} > 0$ if $i = m$. Thus, the diagonal non-zero elements are simply shifted to the right. It can be proved by induction, that the number of non-zero elements increases at least by one during the multiplication by $\mathbf{A}$. Thus, $\mathbf{A}^N$ contains only nonzero elements, where $N \leq m^2 - m$. In the example, $N = 50 < 8^2 - 8 = 56$. The proved property of the transition matrix $\mathbf{A}$ implies that the micro-chaos map is topologically transitive on $\mathcal{A}$.

4. CONCLUSIONS

A two dimensional version of the micro-chaos map was introduced as a simple model of digitally controlled systems. Exploiting the similarity between the well-studied 1D micro-chaos map and the attractor of the 2D map, we proved three properties of this latter map: sensitive dependence on initial conditions, existence of an invariant attractor and topological transitivity. These properties imply that the map (4) is chaotic in finite parameter domains [6].

5. ACKNOWLEDGEMENTS

This research was supported by the Hungarian National Science Foundation under grant no. OTKA F049242, and by the János Bolyai Research Scholarship of the Hungarian Academy of Sciences.

REFERENCES

[1] J. Sieber, B. Krauskopf, "Complex Balancing Motions of an Inverted Pendulum Subject to Delayed Feedback Control", *Physica* **D 197**(3-4), 332-345(2004).

[2] E. Enikov, G. Stépán, "Micro-Chaotic Motion of Digitally Controlled Machines", *J. of Vibration and Control*, **4**, 427-443(1998).

[3] G. Haller, G. Stépán, "Micro-Chaos in Digital Control", *J. Nonlinear Sci.* **6**, 415-448(1996).

[4] G. Csernák, G. Stépán, "Life Expectancy of Transient Microchaotic Behaviour", *J. Nonlinear Sci.*, **15**(2), 63-91(2005).

[5] G. Csernák, G. Stépán, "Quick Estimation of Escape Rate with the Help of Fractal Dimension", *Communications in Nonlinear Science and Numerical Simulation*, **11**(5), 595-605(2005).

[6] S.Wiggins, *Introduction to Applied Nonlinear Dynamical Systems and Chaos*, Texts in Applied Mathematics 2, Springer, New York, 1990.